Phase map by fringe projection with dammann gratings: an application to measure small objects

A. Nava-Vega[a], J. Salinas-Luna[b], E. Luna[c], and J. Manuel Nuñez[c]

[a]*Universidad Autónoma de Baja California, Tijuana, B.C. México,*
e-mail: adriana.nava@uabc.edu.mx
[b]*Universidad del Mar, campus Puerto Ángel, Oaxaca, 70982, México,*
e-mail: jsl@angel.umar.mx
[c]*Universidad Nacional Autónoma de México, Instituto de Astronomía,*
Observatorio Astronómico Nacional, Km. 107 Carretera Tijuana-Ensenada, Ensenada, México, c.p. 22860, México,
e-mail: eala@astrosen.unam.mx, jnunez@astro.unam.mx

The phase of a suitable object was obtained with a fringe projection experiment by using phase shifting with Dammann gratings. As the spacing of the Dammann gratings can be manipulated, it is possible to generate projected thin fringes to improve details of the borders of the object. These gratings have the property that their spacing is not constant, can be programmed, encoded and displayed with versatile performance using a monochromatic source light on a liquid crystal display LCD or by means of a DLP (Digital Light Projector) to develop fringe projection experiments easily and at low cost. As result we have found a high-contrast projection fringes, side and rotation displacements can be better adapted to measure an object. Some fringes images can be generated by fifth order Dammann gratings projected on objects ≤ 20 cm of height.

Keywords: Diffraction; interference multiple; profiling; phase; spatial light modulator.

Empleando la técnica de proyección de franjas se obtiene la fase de objetos, con corrimiento de fase empleando una rejilla binaria Dammann. Debido a que se puede manipular la resolución espacial de las rejillas, podemos modificar el espesor de las franjas que se proyectan y mejorar los detalles de los bordes del objeto. Las rejillas Dammann no tienen un espaciamiento constante, se puede programar y codificar de forma versátil usando luz monocromática a través de una pantalla de cristal líquido LCD, o por medio de un proyector digital de luz DLP para la proyección de franjas, el DLP es una opción de bajo costo y fácil de realizarse. Como resultado, hemos encontrado franjas de alto contraste, los patrones de franjas codificados se pueden girar y desplazar adaptándolas a objetos ≤ 20 cm de altura, En este trabajo se identifica que las rejillas Dammann de orden 5 producen mejores resultados, que se observan en los contrastes de las imágenes obtenidas.

Descriptores: Difracción; interferencia múltiple; perfil; fase; modulador espacial.

PACS: 42.25.Fx; 42.79.Dj; 42.79.Hp; 42.30.-d.

1. Introduction

The purpose of this paper is demonstrate experimentally how to obtain the phase of a small object using a phase shifting algorithm (PS), and a light diffracting element with variable spacing, as is used in the classical Ronchi tests [1]. As advantage in this work, we control the spacing between bands generating thin lines and improving the details of the phase, often used to improve the resolution of the measurement in geometric scope, or with interferometry using monochromatic light sources, a drawback with this option is that the experiment turns expensive. We used an LCD to display fine fringes with Dammann gratings [2], in a fringes projection experiment setup with monochromatic light source. Initially, the quality of the patterns generated by the Dammann gratings was unknown for us; however, we were able to confirm the quality of the projected Dammann fringes for the fringe projection experiment, using a binary grating named Dammann [3], we found that a Dammann gratings in a programmable LCD applied in profilometry technique has not been done. This work is based on the experience gained in Davis laboratory, where was possible to work with interference multiple patterns us-

ing a liquid crystal display (LCD), monochromatic light going through a diffraction Dammann grating [2] producing an interference pattern, of at least two orders of diffraction, generating the width of a line sub-structured in its spatial period; this Dammann grating was mathematically characterized to be displayed on the LCD. In our experiments we generate Dammann gratings with different diffraction orders.

The fringe projection [4] is a non-contact technique, that can be performed either with incoherent or coherent light, illuminating the object with a group of fringes generated by a sinusoidal or binary grating [5,6]. There are some disadvantages with monochromatic light, since this type of illumination induces errors for speckles, produced when light impinges on dust particles on the gratings; in our device we reduced the speckles with optical filters. For incoherent light, digital projectors (DLP) are employed for fringe projection, producing undesired diffraction patterns called pixelation, and increasing when an LCD is used to display gratings of variable frequency [7]. The pixelation produces an effect on high and low frequency images noise, reduced with a composed filter software, that consists of a mixture of frequential and spatial filters, applied to the image where it was at-

tenuated the high-and-medium- frequency noise produced by LCD pixels, without affects the original shape of the fringes, and maintaining the original image intensity [8]. The incorporation of LCD's in optical tests, allows pre-programming of gratings before are deployed [9]. The essential purpose of this work is, to demonstrate experimentally the interference multiple applied to profilometry in a process of selection of diffraction points, generated by Dammann gratings. The advantages of these systems allow lateral displacements, rotations at different angles, and even period variations in real time to observe phase changes in diffraction orders. A secondary objective, is to show the experimental methodology and mathematical theory used to generate and characterize Dammann gratings. In order to test the performance of Dammann gratings in fringe projection with incoherent illumination, we used a digital light projector (DLP) to project and measure an arbitrary object. The experiments on fringe projection with coherent illumination were considered to demonstrate the patterns quality in certains points on the image, such as acceptable definition of the image border, homogeneous intensity and particularly free of border effects. This paper is organized as follows: a Dammann gratings description, design, and programming are presented on Sec. 2. The experimental set-up to generate Dammann gratings is described on Sec. 3. The results and characteristics of dynamic Dammann gratings are presented in Sec. 4. Section 5 presents an application of profilometry with Dammann gratings. Finally, Sec. 6 includes the discussion and conclusions of this study.

2. Dammann gratings

H. Dammann [2] was the first suggested the use of structured binary gratings (or sub-structured Katyl-type gratings [10]). Later, Zhou and Liu [11] improved the grating by generating up to 32 orders of diffraction. The Diffraction Dammann gratings consist of FT- holograms designed to generate an arrangement of point sources with binary phases, values of 0 and π have the same intensity on a remote field. Our work is supported by the physical phenomenon of multiple-interference, according to the well-known Huygens principle [12]. The multiple interference pattern generation is considered to be the N sources points, in our case a number of source points are generated for different orders of the gratings diffraction and are subsequently superimposed; it is quite well-known that an increase of the spatial coherence generates patterns with acceptable contrast. However, unlike lineal sources, Dammann binary gratings have uniform diffracted light intensity.

Fringe projection [4] is a technique where an object is illuminated by a group of fringes with structured illumination which can be performed with coherent or incoherent light. Projected point sources produced by this structured illumination are highly energetic and efficient due to their diffractive properties.

2.1. Generation and calibration of Dammann gratings

In order to generate a Dammann grating, let us first consider a transmission function $t(x)$, of period d, defined by two parts: the first part is valid between $x = 0$ and $x = \omega$ with a transmission value of t_1, whose value remains constant on the given range with a phase value of $\varphi = 0$. For a second part, between $x = \omega$ and $x = d$, the function has a constant transmission value of t_2, and a phase value of $\varphi = \pi$, The transmission function is represented by the relation:

$$t(x) = \sum_{n=-\infty}^{\infty} C_n e^{inx}, \tag{1}$$

where the coefficient C_n is given by,

$$C_n = \frac{1}{d} \int_0^d t(x) e^{-inx\gamma} dx, \tag{2}$$

n is an integer number, and the parameter γ is

$$\gamma = \frac{2\pi}{d}. \tag{3}$$

After taking the Fourier transform of $t(x)$ we obtain:

$$T(p) = \sum_{n-\infty}^{+\infty} C_n(p - n), \tag{4}$$

Where p represents the bright point location, given by,

$$p = \frac{2\pi}{\lambda} \sin \theta = \frac{2\pi}{d} n. \tag{5}$$

Dammann gratings are classified in function of the generated diffraction points, which defines the structure of the Dammann grating. Up to 32 orders of diffraction could be generated according literature [11]. It is observed that the diffraction orders affects projected fringes, producing better sharpness when the order of the fringes increases, assertion verified in Sec. 4. In order to select the order of the grating to be used in this study, intensities of 3, 4, 5, 6, and 7th order
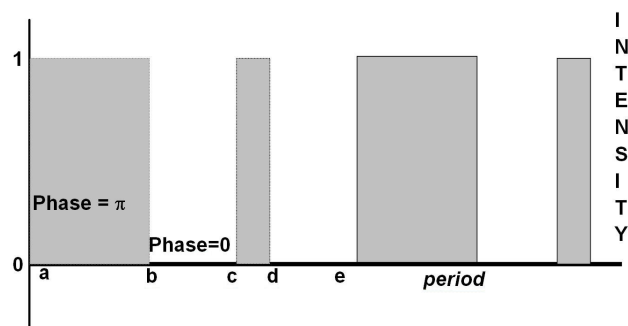
FIGURE 1. Binary gratings schematic diagram with five transitions points a, b, c, d, and e values, in the period p. Intensity is uniform and equal to one. Phase's values are 0 or π.
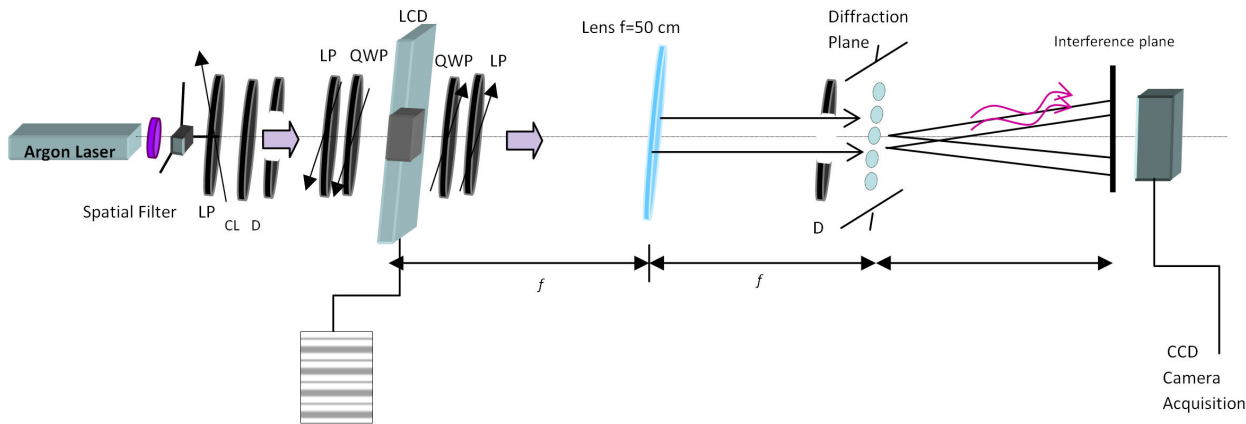
FIGURE 2. Experimental set-up to generate interference multiple patterns with Dammann diffraction gratings. Main component parts: Argon laser, spatial filter, linear polarizer (LP), collimating lens (CL), diaphragm (D), $\lambda/4$ retarding plate (QWP), liquid-crystal display (LCD), a second set of QWP, LP and diaphragm (D); and a CCD camera.

FT-Dammann gratings, were experimentally analyzed. A 5th order grating resulted being the most suitable for our purposes because a grating of this type has an adequate performance derived from change rate defined by δ = *Period grating / Number of pixels*, which is identified of the LCD quality (pixel density), a second reason is that a 5th order grating contains more defined lines than 3, 4, 6, and 7th order gratings on the region of transmission on the LCD. A schematic diagram of the structure of this type of gratings is shown in Fig. 1, where a 5th order grating with five generated points of diffraction are depicted, a Dammann grating in the period (p) provides a structure defined by transitions points. To generate a 5th Dammann order structure, we set numbers, called transition points that defines the binary structure of one period, which have values of $a = 0$, $b = 0.03863$, $c = 0.39084$, $d = 0.65552$, and $e = 1$, defining a value of $p = 1$, considered as the grating period; unlike binary gratings with a period (p), with two values of same width $(w = p/2)$.

Figure 1 shows a Dammann grating, generated by transition points a, b, c, d and e, a fingerprint diffraction pattern with the same values for intensity and phase for its diffraction orders is produced. Thus, in order to design a Dammann grating into an LCD, it is necessary to measure the LCD pixel arrangement and generate the pixel number for each segment of the Dammann grating. From Eq. (2), the values of the coefficients for the transmission function for this particular case are:

$$C_n = \frac{1}{p}\left[\int_0^{0.03863} t(x)e^{-inx\gamma}dx + \int_{0.03863}^{0.39084} t(x)e^{-in\gamma}dx \right.$$

$$\left. + \int_{0.39084}^{0.65552} t(x)e^{-in\gamma}dx + \int_{0.39084}^{1} t(x)e^{-in\lambda}dx \right] \quad (6)$$

After solved, and some simplifications,

$$C_n = -\frac{1}{in\pi}\left\{ [\cos(2n\pi b) - \cos(2n\pi c) + \cos(2n\pi d) - 1] \right.$$

$$\left. + i[-\sin(2n\pi b) + \sin(2n\pi c) - \sin(2n\pi d)] \right\}. \quad (7)$$

With $n = 2$, -1, 0, 1, 2, the coefficients C_n can be represented by, $C_n = (-1/in\pi)[A + iB]$, where A and B are the real and imaginary coefficients, respectively. The intensity of the 5th order Dammann gratings is therefore given by:

$$I = C_n C_n^* = \frac{1}{\pi^2 n^2}[A^2 + B^2]. \quad (8)$$

Equation (9) generates the estimation of the intensity value for each diffraction order, which for this case is equal to 0.7863. Dammann gratings used in this study were programmed with multiple values of δ identifying on this process the best value for the 5th diffraction order grating.

3. Experimental set-up for generating fringe projection with Dammann gratings

Figure 2 shows an optical system set up prepared for generating multiple interference, a coherent laser light from an Argon source ($\lambda = 458$ nm, (for Figs. 4 to 11) expanded and filtered by an objective microscope lens located at a focal distance from a collimator lens (CL) and a diaphragm (D). The device has also a linear polarizer and a density filter to control the incidental light intensity on the LCD (HOLOEYE LC2002). LCD dimensions can be scaled from 800×600 pixels up to 1024×800 pixels. As the main function of the LCD is to modulate the phase of the diffracted light, it is important to achieve its optimal performance [13]. To do it, a linear polarizer (LP) and a retarding quarter plate (QWP) are carefully oriented to the left and right side of the LCD. The gratings to be used are programmed and codified to be displayed on the LCD, which is aligned and located in a perpendicular position to the optical axis to avoid inclination errors (tilt = 0).

a) Dammann 2   (b) Dammann 3

(c) Dammann 5   (d) Dammann 7
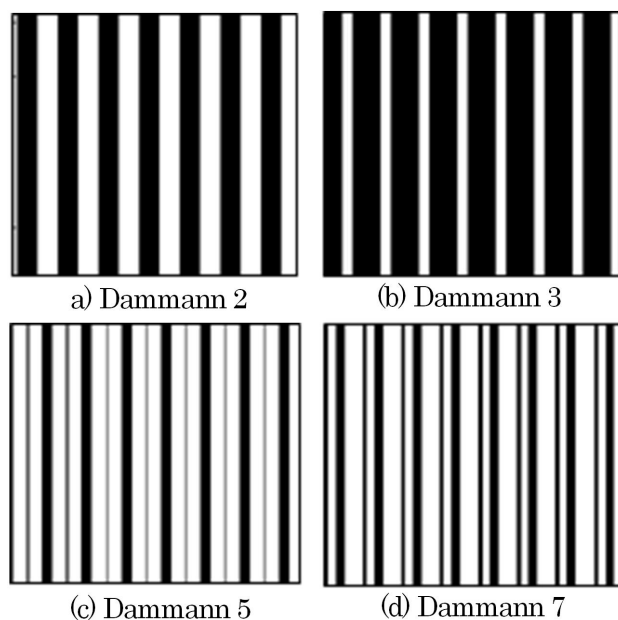
FIGURE 3. Software programmed patterns for 2, 3, 5, and 7th diffraction order Dammann digital gratings, programmed with 13 pixels period.

An optical diffraction pattern with shape of an extended source was generated in the focal distance of a positive lens (focal distance of 50 cm and diameter 5 cm), by using an LCD as light diffuser device. This diffraction pattern is the FT of the Dammann grating displayed by the LCD. Before the generation of diffraction orders at the Fourier plane, the wave front is passed through a diaphragm (D) in order to eliminate some secondary lobes from diffraction orders and speckles due to environment dust. After generating the point sources at the Fourier plane, non-localized bands are generated on the back plane, which can be obtained by adjusting the size of the image impinging on the CCD applying slight camera displacements along the system's optical axis.

4. Results and Discussion

Several experiments were performed to generate Dammann gratings with different diffraction orders, varying the grating's period and adjusting the δ number in the software program. Figure 3 shows different structures bands, which are generated according to the transition point values [11]. An interesting task was to find optimal conditions to attain the highest diffraction orders and to generate remarkable multiple interference patterns. Figure (4a) shows the pattern generated by a 5th order Dammann grating programmed and encoded on the LCD employed (LC2002); diffracted points of the system on the Fourier plane are shown on Fig. (4b), which were captured by a CCD camera, and five intensity peaks are shown at Fig. (4c). It is worth noting that all peaks have the same intensity, and that central peak is slightly higher than the rest, which can be due to transmission bias. An optimal value of δ was determined with a 13 pixel resolution in ac-

(a)

(b)

(c)
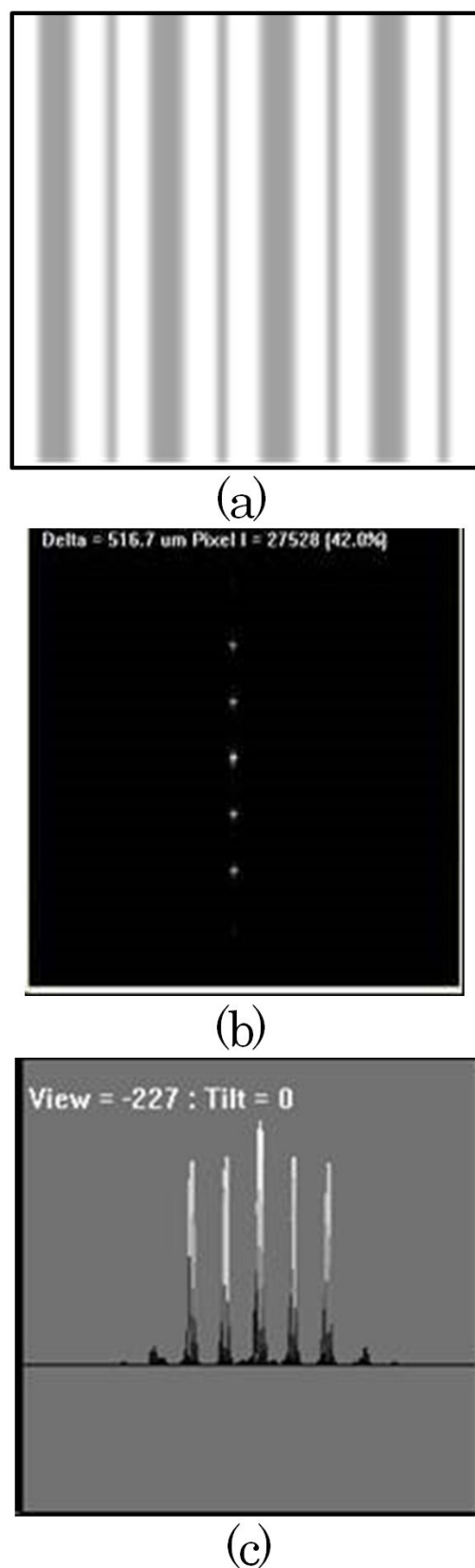
FIGURE 4. Dammann diffraction grating with a 13 pixels' period: (a) Coded digital grating on the LCD; (b) five diffraction points generated and (c) the five points' intensity profile.

(a)　　　　　　　　　　(b)

(c)　　　　　　　　　　(d)
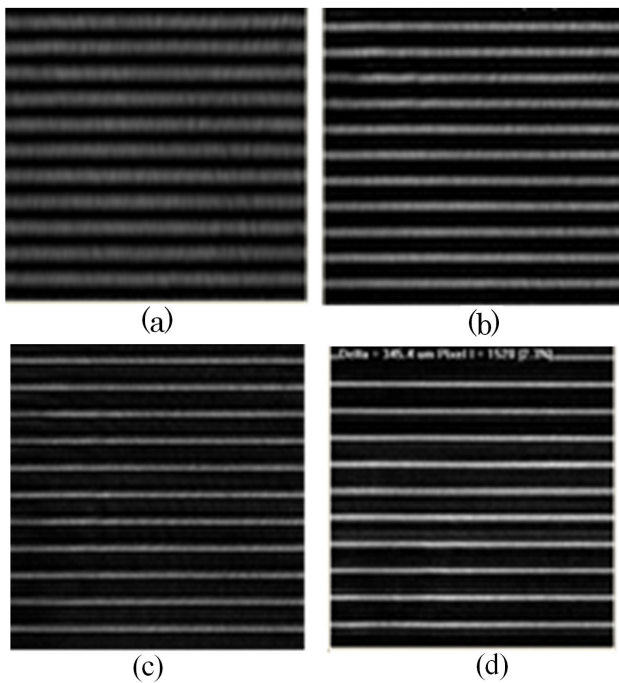
FIGURE 5. Interference patterns generated with optical experimental set up of Fig. 2, with 5th order Dammann grating, a) interference pattern for two diffraction points, (b) 3 diffraction points, (c) 4 points and (d) 5 diffraction points.

(a)　　　　　　　　　　(b)
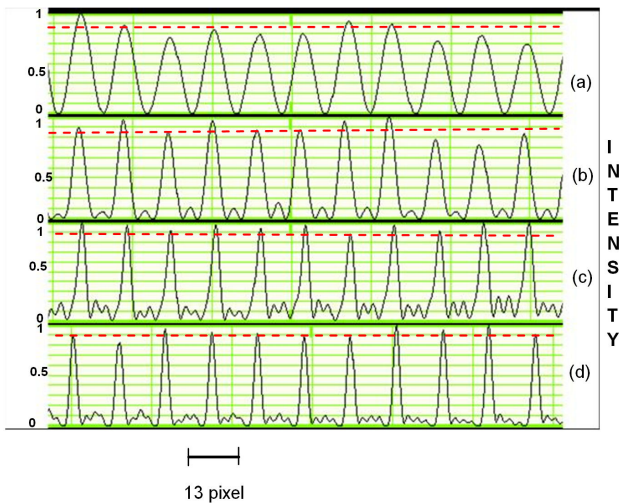
FIGURE 6. Interference multiple profiles generated for (a), (b), (c) and (d) from 2 to 5 filtered diffractions points, using the 5 order Dammann grating with 13 pixel period and $\delta = 78$

cordance with the optical features of the employed LCD, thus it was obtained a 5th order Dammann grating with a high contrast and intensity. The intensity level of the generated Dammann grating had a value of 0.78 as determined by the CCD WinCAM camera's software, value in accordance with the theory [11].

In Fig. 5 we show the contrast behavior in the interference patterns when the diffraction points of the Dammann grating are increased. In (5b), (5c) and (5d), it can be appreciated an extremely fine bands near the central fringe maxi-

(a)　　　　　　　　　　(b)

(c)　　　　　　　　　　(d)

(e)　　　　　　　　　　(f)
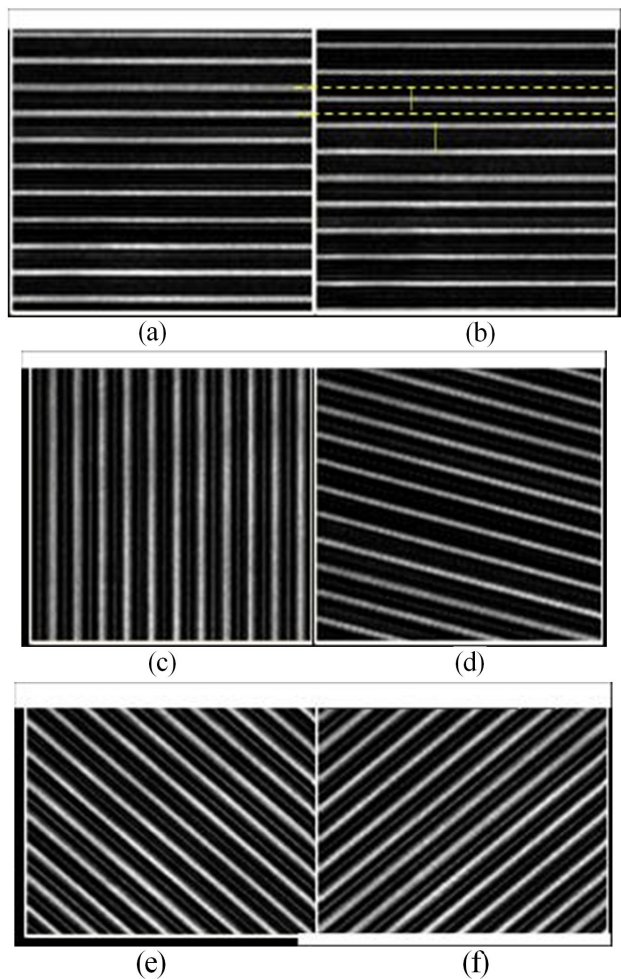
FIGURE 7. Dammann grating (a) Horizontal, (b) Horizontal with half lateral period shifting, c) 90°+, d) +15°-, e) +45°, and (d) -45° rotation.
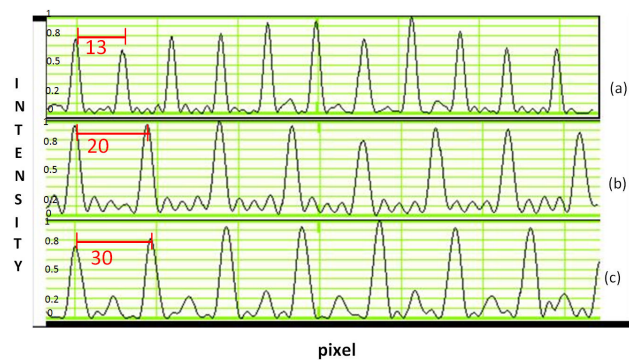
FIGURE 8. Interference multiple profiles for 5 order Dammann grating with (a) δ=78, period of de 13 pixels (intensity peak of 82%), (b) δ= 51, period 20 pixels (intensity peak of 77%), and (c) δ =34, period of 30 pixels (intensity peak 82%).

mum, these are some secondary lobules, even so we still can take advantage of these fine fringes, if we project them on any arbitrary object in order to analyze their deformation. The definition in the interference bands can be also increased if an additional small defocusing of the CCD is accomplished.
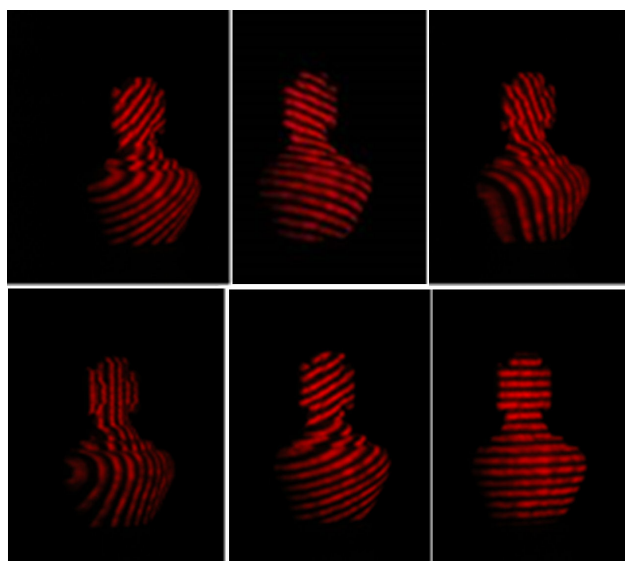
FIGURE 9. Optical patterns of Dammann fringes of order 5. A sequence of orientations for incidental Dammann fringes of order 5, where the fringes are can be vertical, rotated and horizontal.

In our experimental set-up, images of the Dammann fringes obtained are sharper and best defined at 3 cm focus depth, as it is shown at Sec. 5.2 on Fig. (10). Figure 6 shows the interference multiple profiles along the cross section of interferograms of Fig. 5, where we shows the intensity variation of a of (a) two, (b) three, (c) four and (d) five diffraction points, these results satisfy the theory requirements [12], notice that in our case the intensity keeps constant, because the Dammann gratings have this quality. A dotted line at (a), (b), (c) and (d) shows the level with the same value intensity, and slightly deviations at (a) and (b). Some advantages are found when an LCD is used to display the Dammann gratings, because with 3 movements for the gratings we can make a lateral shift, rotation and changes in the fringes period, with this characteristic some phase shifting algorithms can be easy implemented. In Fig. 7 we appreciate the handling of the software in order to generate changes in the optical patterns, in (a) the horizontal fringes images are compared with the image (b) for a pattern where the fringes have been displaced half a period. Results with 90° rotation are shown at (c). Figure (7d) shows a + 15° rotation, and Fig. (7e) and (7f) shows images with rotations of ± 45°, respectively.

A further advantage in this experiment is a period change that can be made in the fringes. At Fig. (8), from (a) to (c) we shows images of interference multiple profile with corresponding δ = 78, 51, 34, generating 13, 20 and 30 pixel period respectively. As Fig. 6, these profiles are obtained taking the cross section of the interferograms generated. We can see in this figure, the displacement of the peaks in relation to the behavior of δ. It is worth to mention that the speckles are the result of the interference of many waves, of the same frequency, having different phases and amplitudes which add together gives a resultant wave whose amplitude, and intensity varies randomly, it is not the case generated for
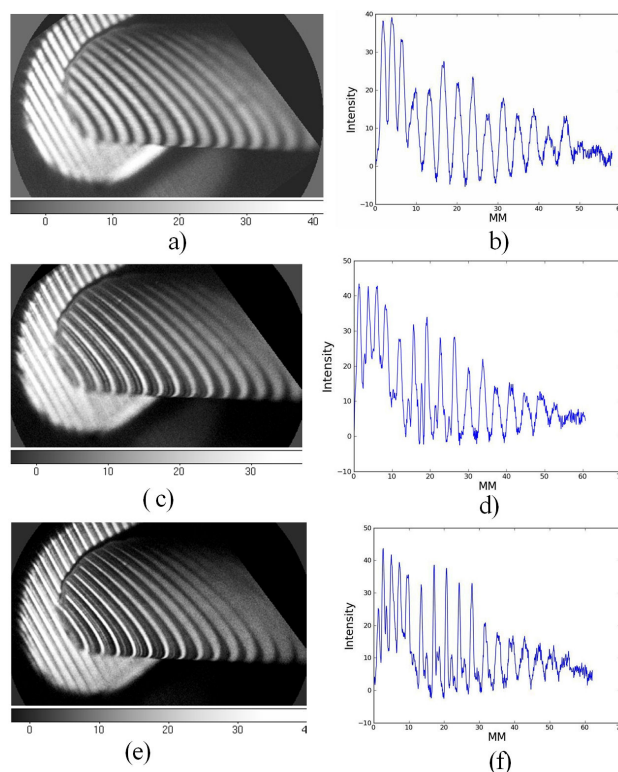
FIGURE 10. Dammann grating order 5. (a) & (b): image with Dammann fringes and intensity variations for 2 diffraction spots, respectively, (c) & (d), and (e) & (f), for 3 and 5 diffraction spots.

Dammann gratings interference, that shows multiple interference patterns with the same intensity level.

5.   Calibration and best focus

In order to assure the absence of pixels effect and speckles on the images, we changed the wavelength and observed if pixel errors appeared on the images. Figure 9 shows a chess piece with a projected light beam of a He-Ne laser with 0.1 m diameter. This image was obtained with the experimental set-up showed in Fig. 2; the pixel effects and speckles are not observed confirming this fact. Dammann fringes are sprained considering the surface characteristics; also it is shown at Fig. 9 that the projected fringes can be rotated on the object for a best characterization in any interesting direction, for further experiments of white light, and Dammann gratings projected with a DLP.

5.1.   DLP Experiment

An incoherent experiment was made in order to analyze the behavior of the projection for Dammann fringes without equivalent wavelength, and with a suitable calibration method. Following the profilometry test, the object phase is measure with white light. We tested another object showing at Fig. (10) the results of the projection focusing process for
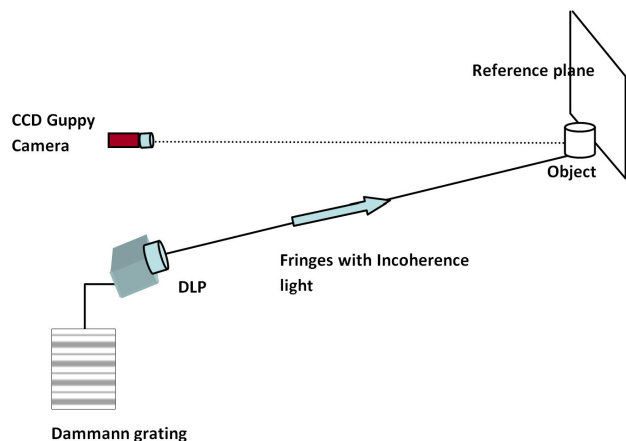
FIGURE 11. Experimental set up in profilometry technique. DLP, object, and CCD camera.
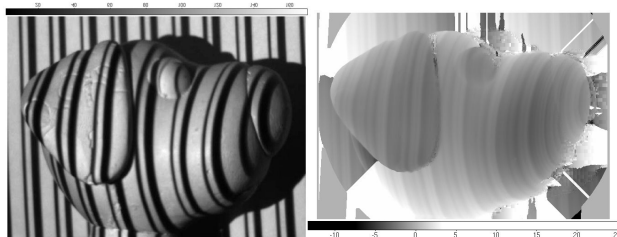
FIGURE 12. a) Dammann fringes projected on the object, b) Phase map obtained.

fine fringes Dammann on the border of a piece of chalk. In this figure the images shows fringes that degrade as they goes out of depth of focus of the system, images (b), (d) and (f) show the distance in question (measured as 3 cm); the Dammann fringes achieves a best definition on the object border by varying the number of spots intensity.

Figure 11 shows the experimental set-up used to reproduce the profilometry technique using a DLP and a CCD Guppy camera with 640×480 pixel array. In this experiment, the Dammann gratings are projected using the DLP. The fringes generated by the Dammann grating are distorted on the object surface; the final image is recorded with the CCD camera. In our experiments, 10 digital images were taken with shifts, which were made through the computer program. An image of a dog head with the Dammann fringes is shown in Fig. (12a) and the corresponding phase in (12b).

The phase map for the plaster dog head was obtained using a deterministic convergence in iterative phase shifting al-

gorithm [14,15] .We notice in this figure that the phase measurement can be obtained in spite of a Dammann grating with sub-structured period was used. This is the first reported work where the phase can be obtained with a sub-structure grating.

6. Conclusions

In this paper, with Dammann gratings we generated fringes applied to profilometry technique. By using Dammann fringes, it is not necessary to develop a binary or sinusoidal grating combination [8]; our method can be defined mathematically for any sub-structured grating that can be used to generate interference fringes. There is a relationship between the diffraction points generated by the interference multiple and the performance of the Dammann fringes. We demonstrated in our experiment that the 5th order Dammann grating has the best performance in profilometry technique, also we demonstrated that the fringe projection can be a dynamic experiment, controlling the period spacing, the orientation and the parameter δ = *Period grating / Number of pixels* of the LCD employed.

We can make phase shifting using software with a great precision without to calibrate the electronic actuators to introduce phase changes. The best feature in the patterns is the excellent definition of the fringes in the borders of the object, the projected fringes appear to be cut abruptly for a knife without showing edge effects and without the pixels effect, see Fig. 10.

Profilometry fringe technique used Dammann gratings as a proof of their feasibility to obtain a phase map, as objects below 20 cm can be measured, we see a great potential of application of this work in the area of Oceanology, in the size measurement of small corals where for its whiteness, the fringes can be projected without affecting the environment where they are.

1. D. Malacara, "*Optical Shop Testing*". John Wiley & Sons, Inc. (2007) ISBN: 978-0-471-48404-2.

2. H. Dammann and E. Klotz, *Opt. Acta* **24** (1997) 505.

3. Jun Zhang, Changhe Zhou, and Xiaoxin Wang, *Applied Optics* Vol. 48, No. 19. (2009).

4. L. Salas, E. Luna, J. Salinas, V. García and M. Servín, *Opt. Eng.* **42** (2003) 3307-3314.

5. E. Stoyka, G. Minchev and V. Sainov, *Applied Optics*, Vol. 48, No. 24. (2009).

6. G.A. Ayubi *et al*., *Applied Optics*, Vol. 50, No. 2, (2011).

7. J. Salinas-Luna *et al*., *Opt. Eng.* **48** (2009) 013604.

8. M. Mora-González *et al,. Proceeding of SPIE*, **8436** (2012) 1-6.

9. C. Quan, J.C. Tay, X.Kang, X.Y. He, and H.M. Shang, *Appl. Opt.* **42** (2005) 2329-2335.

10. R.H. Katyl, *Appl. Opt.* **11** (1972) 2278-2285.

11. Ch. Zhou, and L. Liu, *Applied optics*, vol. 34, No. 26 (1995).

12. E. Hecht, "*Optics*", Pearson Addison Wesley (2002).

13. J.A. Davis, J. Nicolás, and A. Marquez, "*Phasor analysis of eigenvectors generated in liquid-crystal displays*". 1 August 2002/ Vol. 41, No. 22/ *Applied Optics*, / Vol. 41, No. 22/ 1 August 2002.

14. E. Luna, L. Salas, E. Sohn, E. Ruiz, J.M. Nuñez, and J. Herrera, *Appl. Opt.* **48** (2009) 1494-1501.

15. J. Herrera, E. Luna, L. Salas, E. Sohn, and E. Ruiz, *Appl. Opt.* **52** (2013) 1913-1918.